

MALAYSIAN JOURNAL OF ANALYTICAL SCIENCES



Journal homepage: https://mjas.analis.com.my/

Research Article

Structural and electrical properties of chitosan grafted polyvinyl acetate (Ch-g-PVAc) with lithium triflate-based polymer electrolytes

Ain Sorhana Nabila Ismadi¹, Nor Kartini Jaafar^{1*}, Mohd Zaki Mohd Yusoff², and Rosnah Zakaria¹

Received: 14 October 2024; Revised: 25 January 2025; Accepted: 14 February 2025; Published: 13 April 2025

Abstract

Solid polymer electrolytes (SPEs) based on natural polymers are gaining attention due to their environmentally friendly, biodegradable, biocompatible, and safer materials compared to liquid electrolytes. Numerous studies have been conducted to develop polymer electrolytes with enhanced conductivity and long-term safety. In this study, chitosan-based natural solid polymer electrolytes with polyvinyl acetate (PVAc) using graph copolymerisation were studied. The polymer system of grafted Ch-g-PVAc with different concentrations of lithium triflate (LiTf) salt was successfully prepared using solution casting method. The X-Ray diffraction (XRD) revealed the reduction in the crystalline nature upon the inclusion of LiTf. Fourier transform infrared spectroscopy (FTIR) analysis revealed that the PVAc was successfully grafted onto the chitosan backbone, and the interaction of LiTf with Ch-g-PVAc are confirmed by the existence of several functional groups. The bulk resistance decreases with increasing salt content which is shown in electrical impedance spectroscopy (EIS) result. The highest ionic conductivity, 6.68×10^{-5} S cm⁻¹ was obtained for Ch-g-PVAc doped with 50 wt.% LiTf salt with a breakdown voltage of 3.5 V as measured by Linear Sweep Voltammetry (LSV). This study proposes an environmentally friendly and practical electrolyte with excellent electrochemical performance suitable for the development of electrochemical devices.

Keywords: Chitosan, Ch-g-PVAc, poly(vinyl) acetate, lithium triflate, amorphous

Introduction

Solid polymer electrolytes (SPEs) have gained significant interest as substances used in various electrochemical devices such as batteries, fuel cells, polymer sensors. and supercapacitors. The electrolytes associated with lithium salt and incorporated into neutral polymer have been developed as replacements for liquid electrolytes in lithium-ion batteries. SPEs possess ion transport properties similar to those of common liquid solutions while being safer, less toxic, and lighter. Recently, bio-polymer electrolytes have received attention due to its eco-friendly, cost-effective, biodegradable, and biocompatible polymer. The main characteristics required for the development of polymer electrolytes include high room temperature conductivity and good mechanical stability [1]. Due to its excellent characteristics, such as the ability to form a strong film and high hydrophilicity, chitosan

(Ch) has been chosen as a host polymer for this polymer studies. Chitosan is the second most abundant polysaccharide in nature and is derived from chitin through deacetylation with an alkali [2]. This process of deacetylation removes acetyl groups from the molecular chain of chitin, leaving behind amino groups and replacing them with hydroxyl groups [3]. Chitosan contains free amine groups and various oxygen groups with lone-pair electrons [4] which enhanced tendency to have affinity interactions with dopants. The presence of polar functional groups in chitosan imparts a dipole moment to the materials which influenced the dielectric polarisation [5]. In biodegradable SPEs, the amorphous regions of the host polymer matrix are conductive to ion conduction whereas most biopolymers inherently possess a semi-crystalline nature [6]. Biopolymer such chitosan, which contains high levels of electron donor atom can be combined

¹School of Physics and Material Studies, Faculty of Applied Sciences, Universiti Teknologi MARA (UiTM), 40450 Shah Alam, Selangor, Malaysia

²Institute for Biodiversity and Sustainable Development (IBSD), Universiti Teknologi MARA, 40450 Shah Alam, Selangor, Malaysia

^{*}Corresponding author: norka603@uitm.edu.my

with the synthetic polymer or incorporated into composites [7].

On the other hand, polyvinyl acetate (PVAc) is a synthetic polymer with an amorphous state which helps to decrease the crystallinity of the host polymer [8]. PVAc is highly soluble in common organic and exhibits excellent solubility. Additionally, the salt doping method is a promising method to increase ionic conductivity at room temperature. Based on previous study, lithium-based polymers demonstrate overall good performance in essential characteristics, with ionic conductivity reaching 8.37 x 10⁻⁴ Scm⁻¹ for 1 TSP (tamarind seed polysaccharide) and 0.45 g LiCF₃SO₃ [9] Numerous research efforts have focused on copolymerisation involving chitosan and other polymers, to address certain drawbacks, such as inadequate mechanical strength, limited thermal resistance, and low selectivity as an adsorbent [10]. Chitosan typically serves as the backbone chain in grafting method due to its high molecular weight. However, chitosan has low ionic conductivity and high hydrophilicity. Most copolymers are synthesised by grafting vinyl monomers onto the chitosan backbone [11]. The grafting of chitosan allows the formation of covalent binding onto the chitosan backbone. Various techniques are available to initiate graft copolymerisation, including electromagnetic radiation such as gamma rays, UV light, and free radical initiators [12]. Gamma rays are particularly effective as they can penetrate and break the chemical bonds of chitosan backbone, create free radicals. The free radicals facilitate the formation of covalent bonds between the chitosan and PVAc.

Additionally, the addition of an appropriate quantity of lithium salt to the polymer matrix significantly improves the ionic conductivity of the polymer electrolyte by increasing the number of charge carriers, thereby providing free ions for conduction [13] therefore lithium triflate was chosen as salt in this study. According to the Kingslin Mary Genova et., 2017 [14], the maximum ionic conductivity of PVA-PAN with 50 wt.% of LiCF₃SO₃ is at 4.0 x 10⁻⁵ Scm⁻¹ and Jannah et al. [15] reported that LiTfdoped-pectin based has highest conductivity at 3.87 x 10⁻⁵ Scm⁻¹. Both of this study demonstrated that adding salt such as lithium triflate into the polymer electrolyte can enhance ionic conductivity, achieving up to 10^{-5} S cm⁻¹ with 50 wt.% LiTf. However, this current study indicates that while 50 wt.% LiTf remains optimal, a substantial improvement in ionic conductivity is observed when vinyl acetate (VAc) is introduced through graft copolymerisation. The development of grafted PVAc onto chitosan backbone has not been much studied by researchers.

This study aims to develop polymer electrolytes based on Ch-g-PVAc with varying concentrations of LiTf salt by solution casting technique. The prepared SPEs were characterised by the X-Ray diffraction (XRD), which confirms the amorphous nature of the polymer electrolyte while FTIR was used to confirm the interactions between salt and grafted polymer matrix. The highest conducting electrolyte was further analysed for its breakdown voltage using linear sweep voltammetry (LSV).

Materials and Methods Sample preparation

Grafted polymer electrolytes were synthesised by graft co-polymerising vinyl acetate (VAc) onto chitosan using a simultaneous gamma (γ) radiation technique. Chitosan was dissolved in 1% acetic acid and stirred overnight until completely dissolved with no heat required during the stirring process. This was followed by the addition of vinyl acetate (VAc) solution, and the mixture was stirred until fully dissolved with no heat required during the stirring process. The resulting solution was then exposed to gamma irradiation using a Cobalt-60 source at the One Stop Gamma Sterilizing Center, SINAGAMA, Malaysian Nuclear Agency (NUCLEAR MALAYSIA). The grafted sample solution was poured into a Teflon dish and left to form a grafted chitosan-PVAc film at room temperature. The grafted copolymer film was subsequently dried under vacuum conditions at 50°C until a constant weight was obtained. Next, the Ch-g-PVAc polymer was introduced into a 1% acetic acid solution and stirred overnight until completely dissolved with no heat required during the stirring process. The Ch-g-PVAc solution was then separately doped with various concentrations of lithium triflate (LiTf) salt (0 wt.%, 10 wt.%, 20 wt.%, 30 wt.%, 40 wt.%, and 50 wt.%) as detailed in Table 1. Each sample was poured into individual Teflon dishes and allowed to form a Ch-g-PVAc-LiTf film at room temperature as shown in Figure 1. The films were subsequently placed in a silica gel desiccator to further dry and eliminate any remaining moisture.

Table 1. Composition of Lithium Triflate salt

Designated	Ch-g- PVAc (g)	Lithium Triflate (g)	Lithium Triflate (wt.%)
S1	1.00	0	0
S2	0.90	0.10	10
S3	0.80	0.20	20
S4	0.70	0.30	30
S5	0.60	0.40	40
S6	0.50	0.50	50

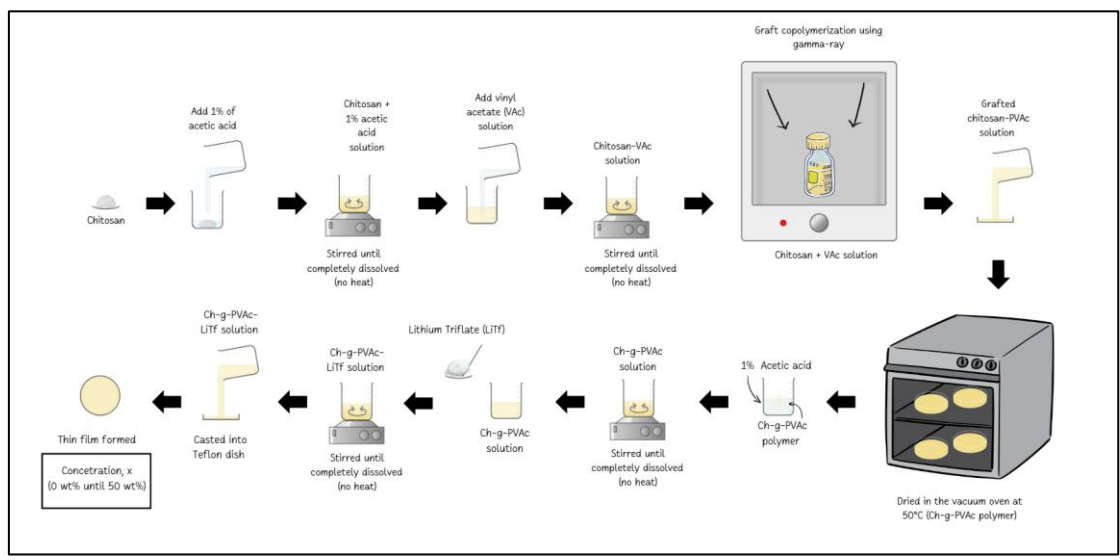


Figure 1. Preparation of grafted polymer electrolytes (Ch-g-PVAc-LiTf)

Characterisation of polymer electrolyte

The physical properties of SPEs were assessed based on water absorption. Water uptake was used to determine the hydrophilicity of chitosan before and after graft copolymerisation. Water uptake was

calculated using Eq (1).

$$Water uptake = \frac{Wwet-Wdry}{Wdry} X 100\%$$
 (1)

Where W_{dry} is the initial weight of the sample and W_{wet} is the final weight of the sample after being soaked in water for 24 hours. XRD was employed to examine transitions in crystallinity and the amorphous structure of Ch-g-PVAc with salt polymer electrolyte. The analysis was conducted using an X'Pert PRO, PAN Analytical, DY2536 instrument at the Faculty of Applied Sciences, UiTM Shah Alam, covering a wide 2θ range ($5 \le 2\theta \le 60$) at room temperature. FTIR was utilised to investigate the interaction between the Ch-g-PVAc polymer and the LiTf salt. Spectra were recorded in the wavenumber range of 650 to 2000 cm⁻¹ in transmittance mode at 303 K (room temperature). The electrolyte film was positioned between two stainless steel (SS) electrodes. The impedance spectrum was performed using a HIOKI Impedance Tester located at the IMADE laboratory, Institute of Science (IOS), to study the ionic conductivity of the grafted polymer with salt. The frequency range for EIS analysis was from 100 Hz to 1 MHz, employing stainless steel electrodes.

The ionic conductivity was calculated using Eq (2)
$$\sigma = \frac{t}{R_{h}A}$$
 (2)

Where t is the thickness of the thin film, R_b is the

bulk resistance and A is the surface area of the electrolytes. The bulk resistance (R_b) was obtained based on the results of electrical spectroscopy using the plot's intercept of the semicircle arc on the real axis (Z_r) at high frequency region [2]. From the EIS analyses, dielectric constant and dielectric loss also were calculated from the Z_r and Z_i parts where Z_r and Z_i represents the real and imaginary parts respectively of the complex impedance (Z*) using Eq (3) and Eq (4)

$$\varepsilon' = \frac{Z_i}{\omega C_0(Z_r^2 + Z_i^2)} \tag{3}$$

$$\varepsilon' = \frac{Z_i}{\omega C_0(Z_r^2 + Z_i^2)}$$

$$\varepsilon'' = \frac{Z_r}{\omega C_0(Z_r^2 + Z_i^2)}$$
(4)

Where Co is the vacuum capacitance which is equivalent to $\varepsilon_0 = A/t$ where ε_0 is permittivity of free space (8.85 x 10⁻¹² F/m). LSV analysis was conducted at a sweep rate of 5 mVs⁻¹ across a potential range of 0 - 4.2 V.

Results and Discussion Water uptake analysis

Figure 2 shows the water uptake for pure chitosan and chitosan grafted poly(vinyl acetate), Ch-g-PVAc. The result indicates a significant decrease in the water uptake after grafting poly(vinyl acetate) onto the chitosan backbone. The water uptake for pure chitosan was measured at 3.15% whereas for Ch-g-PVAc, it was 0.68%. This reduction of hydrophilicity of chitosan helps to improve the mechanical and electrochemical stabilities thereby enhancing ionic conductivity. Excessive water absorption potentially damage the cathode membranes [16]. This grafting method effectively addresses the issue of swelling and tailoring the hydrophilicity of chitosan which is important for achieving optimal SPE performance.

Malays. J. Anal. Sci. Volume 29 Number 2 (2025): 1382

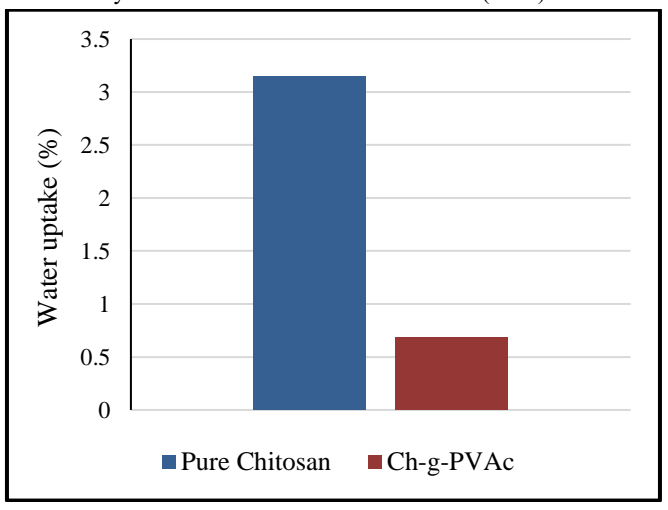


Figure 2. Water uptake for pure chitosan and Ch-g-PVAc

X-ray diffraction (XRD) analysis

The XRD patterns of pure chitosan and Ch-g-PVAc polymer with different concentrations of lithium triflate (LiTf) salt at room temperature are shown in Figure 3. According to Figure 3, chitosan exhibited two significant peaks approximately at $2\theta = 9.94^{\circ}$ and 20.10°. The presence of these crystalline peaks is due to the intermolecular and intramolecular of hydrogen bonding in chitosan. The intensity of the peaks at $2\theta = 9.94^{\circ}$ and 20.10° decreases and broadens due to presence of PVAc after grafted [8]. This shows that the inclusion of PVAc into the chitosan backbone enhances as evidenced by the reduction in crystallinity peaks observed in the XRD results. The decreased intensity of the crystalline peaks further supports the reduced degree of crystallinity in the electrolytes. Upon the addition of LiTf salt, the intensity of the diffraction peak decreases and broadens as illustrated in Figure 3. This reduction in crystallinity of chitosan is due to the LiTf disrupting the chitosan structure, as the lithium ions interact with the polymer chains. Additionally, the broad peak at $2\theta = 9^{\circ}$ - 21° of pure chitosan becomes less pronounced in intensity and increasingly broad, indicating an increase of the amorphous nature of the polymer electrolyte due to LiTf inclusion. In the amorphous state, polymer chains exhibit greater flexibility compared to the crystalline state, leading to enhanced segmental mobility of the polymer chain by providing a larger free volume [17]. This increased flexibility provides better ion transport pathways. Consequently, both mobility and ion concentration contributions increase with higher salt concentrations. Specifically, the polymer composition of Ch-g-PVAc-50 wt.% LiTf is observed to be a highly amorphous structure. This indicates complete dissociation of the salt within the host polymer, forming polymer-salt complexes.

Fourier transform infrared spectroscopy (FTIR) analysis

FTIR was used to analyse the shifting of bands, changes in intensity and the existence of new peaks resulting from the complexation between pure chitosan, Ch-g-PVAc, and lithium triflate salt. Figure 4a and 4b shows the vibrational band values from FTIR spectra of pure chitosan and chitosan-gpolyvinyl (acetate) with various concentrations of lithium triflate (LiTf) salt respectively. Chitosan shows characteristic absorption peaks at 1652 cm⁻¹, 1589 cm^{-1} , 1422 cm^{-1} , 1379 cm^{-1} , 1254 cm^{-1} , 1152cm⁻¹, 1070 cm⁻¹ and 1033 cm⁻¹. The absorption observed at 1652 cm⁻¹ (C=O stretching, Amide I), 1589 cm⁻¹ (N-H bending, Amide II) and 1422 cm⁻¹ (C-H bending, Amide group II) are attributed to its amide group [18]. After graft polymerization with PVAc, a new absorption peak appears at 1730 cm⁻¹ due to the ester group from the PVAc chains as shown in **Figure 4b** [12]. The presence of new bands in the chitosan-g-polyvinyl acetate suggests that PVAc was successfully grafted onto the chitosan backbone. The absorption peak at 1730 cm⁻¹ shifts to the lowest wavenumber and broadens upon the addition of lithium triflate (LiTf) salt at 1729 cm⁻¹, 1719 cm⁻¹, 1720 cm⁻¹, 1719 cm⁻¹ and 1718 cm⁻¹ of concentrations at 10 wt.%, 20 wt.%, 30 wt.%, 40 wt.% and 50 wt.% respectively. This indicates that complexation between the polymer and salt had occurred. The presence of new peaks and the shifts in FTIR peak confirm the complexation of the salt and host polymer. The band at 1033 cm⁻¹ in pure chitosan attributed to C-O stretching, shifts to 1019 cm⁻¹, 1021 cm⁻¹, 1022 cm⁻¹, 1029 cm⁻¹ and 1023 cm⁻¹ for LiTf concentrations of 10 wt.%, 20 wt.%, 30 wt.%. 40 wt.% and 50 wt.% respectively. This shifts may due to the formation of ion pairs and aggregates of $v_s(SO_3)$ (the symmetric stretching mode of bands),

causing the band at $1033~\rm cm^{-1}$ bands to shift to lower wavenumbers and decrease in intensity [1]. The broad band further shifts to a lower number at $1247~\rm cm^{-1}$ as the percentage of LiTf salt increases in the mixture, potentially due to the wave number of V_{as} (SO₃) and V_{s} (CF₃) of the salt [1]. The ester band of PVAc shifts to a lower wave number at $1720~\rm cm^{-1}$

with reduced intensity upon lithium salt incorporation. The presence of peaks in the FTIR spectra and the shift in the polymer peaks provide clear indications of ionic salt forming complexes with the polymers. All the functional group observed was summarised in **Table 2**.

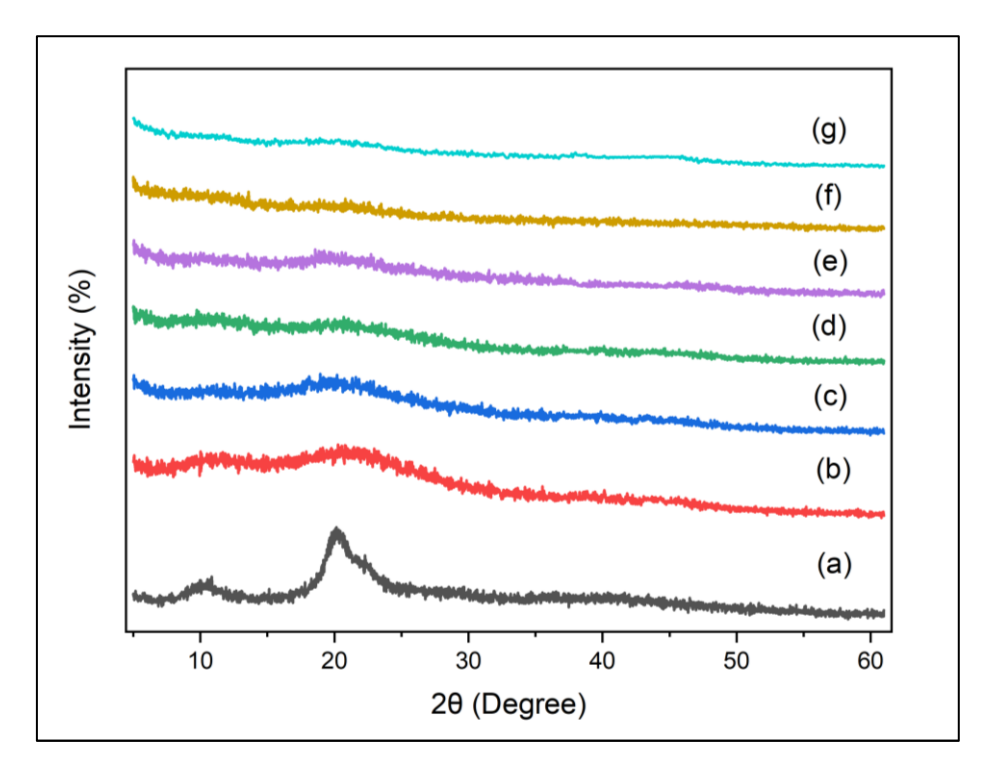
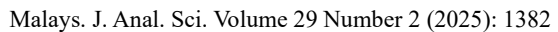
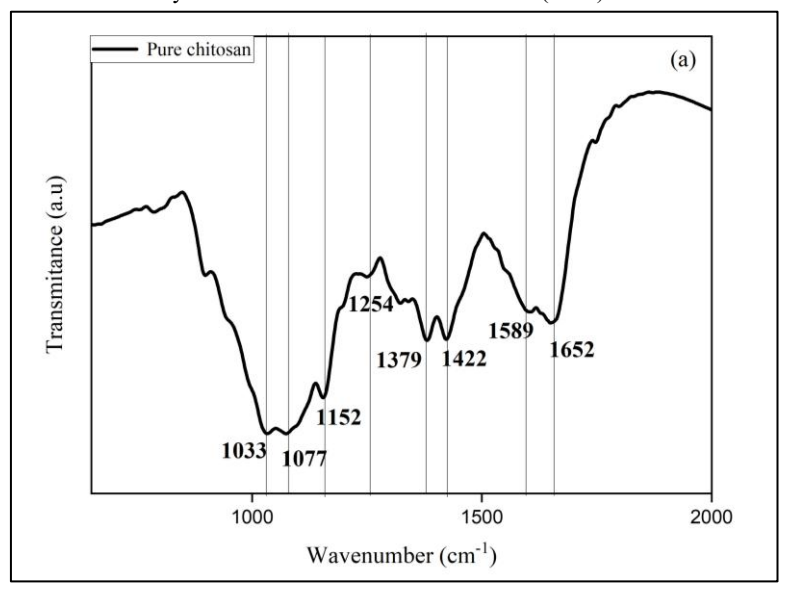


Figure 3. XRD pattern of (a) pure chitosan (b) Ch-g-PVAc-0wt% LiTf (c) Ch-g-PVAc-10wt% LiTf (d) Ch-g-PVAc-20wt% LiTf (e) Ch-g-PVAc-30wt% LiTf (f) Ch-g-PVAc-40wt% LiTf (g) Ch-g-PVAc-50wt% LiTf

Table 2. The functional group observed from FTIR spectra

Description of vibrational modes	Wavenumbers (cm ⁻¹)						
	PC	S1	S2	S3	S4	S5	S6
C=O stretching (Amide I)	1652	1638	1653	1644	1642	1642	1639
N-H bending (Amide II)	1589	1555	1548	1562	1564	1560	1560
CH ₂ bending	1422	1415	1429	1408	1426	1422	1422
C=O stretching (ester group)	-	1730	1729	1719	1720	1719	1718
C-O-C asymmetric stretching	1152	1157	1155	1165	1160	1173	1169
C-O stretching	1033, 1070	1033,1068	1019	1021	1022	1029	1023
CH ₃ bending	1379	1378	1369	1369	1378	1380	1379
C-N stretching (Amide III)	1254	1251	1235	1237	1242	1252	1250





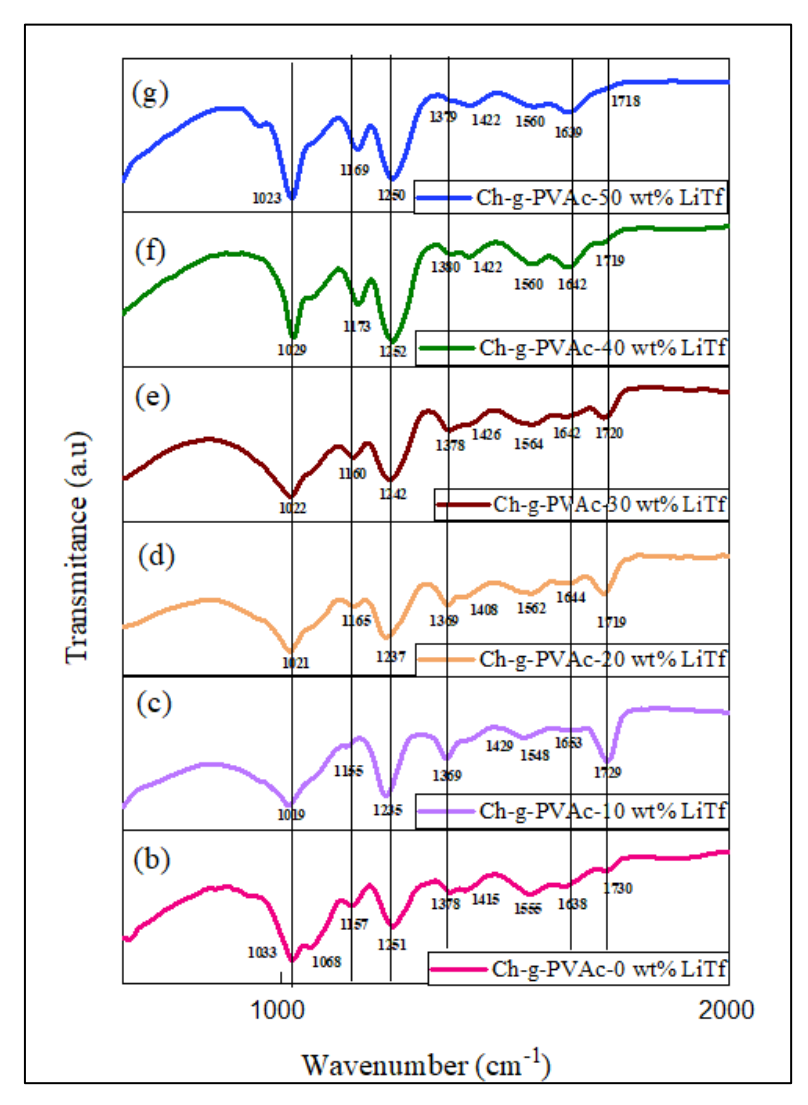


Figure 4. (a) pure chitosan (b) Ch-g-PVAc-0 wt.% LiTf (c) Ch-g-PVAc-10 wt.% LiTf (d) Ch-g-PVAc-20 wt.% LiTf (e) Ch-g-PVAc-30 wt.% LiTf (f) Ch-g-PVAc-40 wt.% LiTf and (g) Ch-g-PVAc-50 wt.% LiTf

Electrical impendence spectroscopy (EIS) analysis Electrical Impedance Spectroscopy (EIS) was analyse the electrical properties of the grafted polymer with salt at room temperature (303 K). Figure 5 represents the pure chitosan and Ch-g-PVAc with various concentrations of lithium triflate salt (0 to 50 wt.%) at room temperature. Based on the formula in Eq (2), ionic conductivity increases as the bulk resistance decreases. The calculated ionic conductivity values of grafted Ch-g-PVAc with different concentrations of lithium triflate salt are shown in Table 3. The ionic conductivity is influenced by the amount of salt incorporated into the polymer matrix and its extent of dissociation. [19]. According to Figure 5, ionic conductivity improves with the addition of salt, reaching its maximum of 50 wt.% lithium triflate salt. Table 3 shows that a low lithium triflate concentration leads to low conductivity due to the limited number of free charge carriers in the electrolytes. As observed in **Table 3**, the conductivity has increased from 10⁻¹⁰ to 10⁻⁵ Scm⁻¹ due to the number of ions increasing as the concentration of lithium triflate salt increases, leading to a higher ionic conductivity. This is attributed to the rising number of ion dissociations as LiTf efficiently dissociate into Li⁺ and Tf, significantly increasing the number of free charge carriers. This shows that adding salt enhances the amorphous state and the number of mobile ions. Furthermore, the increase in amorphous state reduces crystallinity, facilitating swift ion movement as shown in the XRD findings. Additionally, higher salt concentrations boost the amorphous nature, potentially improving the polymer chain's segmental mobility [20]. The polymer chains facilitate the transport of Li⁺ through segmental motions. Consequently, both mobility and ion concentration escalate with higher salt concentrations. It is noteworthy that the addition of salt of 0 wt.% to 50 wt.% causes a significant decrease of Rb from 2.71 x 10⁵ Ohm for Ch-g-PVAc-0 wt.% LiTf to 4.4 x 10¹ Ohm for Ch-g-PVAc-50 wt.% LiTf. Thus, salt effectively improves both carrier number and ionic mobility in the electrolyte systems. Hence, the highest ionic conductivity observed in this study was for the Ch-g-PVAc-50 wt.% LiTf, with a value of 6.68 x 10⁻⁵ Scm⁻¹.

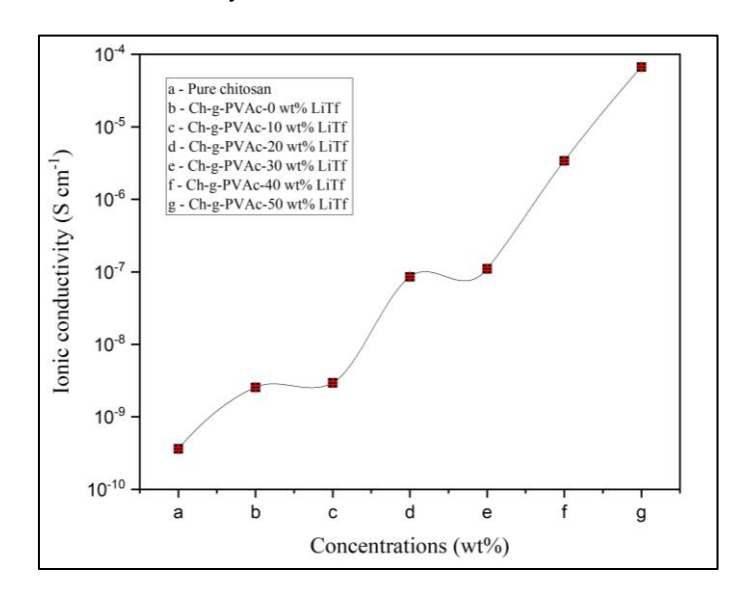


Figure 5. Ionic conductivity for (a) pure chitosan (b) Ch-g-PVAc-0 wt.% LiTf (c) Ch-g-PVAc-10 wt.% LiTf (d) Ch-g-PVAc-20 wt.% LiTf (e) Ch-g-PVAc-30 wt.% LiTf (f) Ch-g-PVAc-40 wt.% LiTf and (g) Ch-g-PVAc-50 wt.% LiTf

Table 3. Ionic conductivity of Ch-g-PVAc with different weight percent of lithium triflate salt at room temperature

Sample Designation	Bulk Resistance (Ω)	LiTf (wt.%)	LiTf (g)	σ (Scm ⁻¹)
Pure chitosan	5.434×10^6	0	0	3.615 x 10 ⁻¹⁰
S1	3.315×10^5	0	0	2.547 x 10 ⁻⁹
S2	6.018×10^5	10	0.10	2.937 x 10 ⁻⁹
S3	2.368×10^4	20	0.20	8.544 x 10 ⁻⁸
S4	1.885×10^4	30	0.30	1.104×10^{-7}
S5	8.855×10^2	40	0.40	3.394 x 10 ⁻⁶
S6	4.408×10^{1}	50	0.50	6.683 x 10 ⁻⁵

Linear sweep voltammetry (LSV) analysis

The maximum potential limit of an electrolyte can be determined using LSV analysis, which is crucial for energy devices research. The LSV analysis with the highest conductivity of Ch-g-PVAc-50 wt.% LiTf. Figure 6 presents the current-voltage graph, from which the breakdown voltage of the electrolyte can be measured. The current exhibits greater stability at lower potential. Based on Figure 6, the electrochemical stability of Ch-g-PVAc-50 wt.% LiTf is approximately at 3.5 V. However, when the potential reaches 3.5 V, the electrolyte reaches its decomposition potential, as indicated by a significant increase in current values. There is no current flow between 2.25 and 3.0 V, suggesting that there are no electrochemical reactions occurring within this potential range. The rise in current beyond 3.5 V was associated with the breakdown of the polymer electrolyte, signifying an electrochemical reaction within the polymer electrolytes [21]. As the potential exceeds 3.5 V, rapid changes in current, from 0.00025 to 0.00033 A are observed. The findings demonstrate that the electrolyte examined in this study can withstand the operational voltage requirements of energy storage devices.

Dielectric constant and loss properties Analysis

The dielectric constant and dielectric loss were calculated using Eq (3) and Eq (4), and their values are plotted in Figure 7 and Figure 8, respectively. As illustrated in previous XRD and FTIR analyses, increasing the amount of LiTf resulted in a reduction in the crystalline area. The dielectric constant and dielectric loss are generally higher at lower frequency and decrease with increasing frequency. This phenomenon can be attributed to the accumulation of charge carriers, or space charge polarisation at the interface between electrode and electrolyte. In other words, reducing the frequency of the applied electric field extends the time for charge carriers to move, raising both the dielectric constant and dielectric loss [22]. Thus, this process has the potential to produce significant polarisation and a high dielectric constant [23]. The rise in dielectric constant with salt concentration suggests an elevation in the concentration of charge carriers, leading to an increase in ionic conductivity. This suggests a high dielectric constant inhibits crystal growth and reduces ion-ion interactions [24].

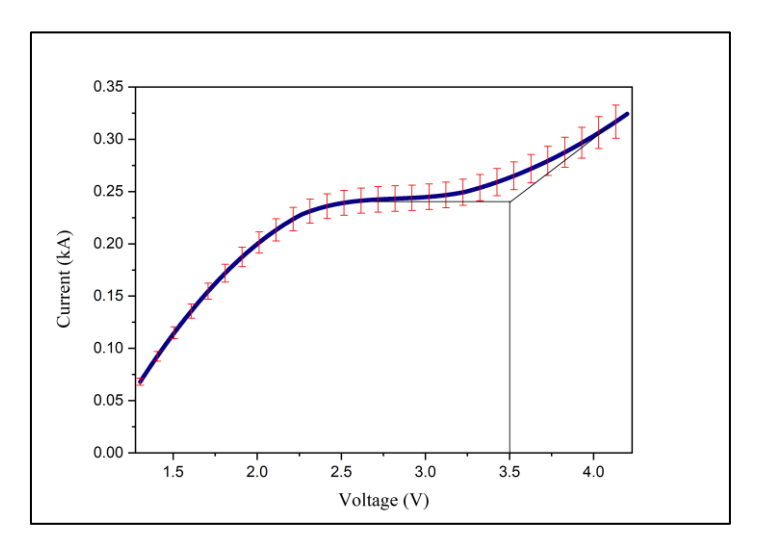


Figure 6. LSV for highest conducting at 5 mVs⁻¹

Malays. J. Anal. Sci. Volume 29 Number 2 (2025): 1382

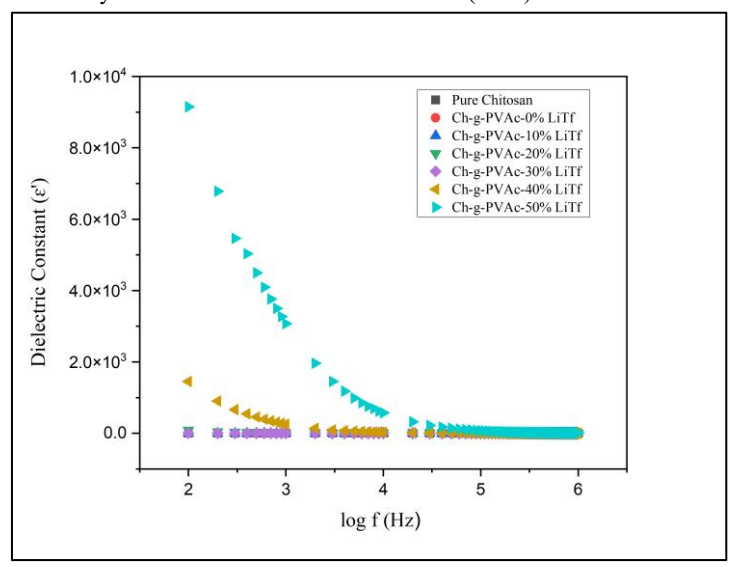


Figure 7. The plot of dielectric constant

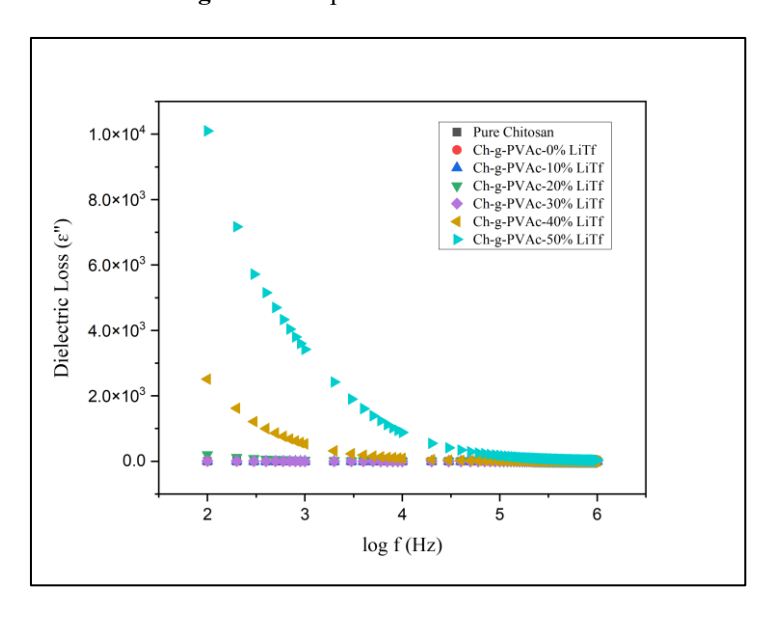


Figure 8. The plot of dielectric loss

Conclusion

In summary, this study developed a novel of Ch-g-PVA polymer electrolyte with various concentrations of LiTf salt. The Ch-g-PVAc-LiTf was characterised using different techniques such as XRD, FTIR, EIS, and LSV. The XRD and FTIR techniques were performed to identify the structural of grafted Ch-g-PVAc, while the EIS and LSV were used to evaluate its electrical properties and window stability respectively. The grafting of Ch-g-PVAc was successfully achieved at different concentrations of LiTf. The XRD analysis revealed the changes in crystallinity and an increase in the amorphous nature of the Ch-g-PVAc-LiTf polymer. Specifically, the polymer composition of Ch-g-PVAc-50 wt.% LiTf was observed to be highly amorphous. This indicates

complete dissociation of the salt within the host polymer in the polymer-salt complexes. FTIR spectroscopy shows the complexation between the Ch-g-PVAc polymer and lithium triflate (LiTf) salt. The presence of peaks in the FTIR spectra and shift in the polymer peaks suggest a clear indication of the ionic salt forming complexes with the host polymer. Among the tested samples, the Ch-g-PVAc polymer electrolyte containing 50 wt.% of LiTf exhibited the highest ionic conductivity at $6.68 \times 10^{-5} \text{ Scm}^{-1}$ at room temperature. This enhancement in conductivity can be attributed to the increased ion mobility and the greater number of charge carriers. According to LSV analysis, the Ch-g-PVAc polymer with 50 wt.% LiTf demonstrated electrochemical stability up to 3.5 V. The addition of 50 wt.% LiTf salt produced the

most favourable results, achieving a five-order-of-magnitude increase in conductivity.

Acknowledgement

The authors express their gratitude to the staff of the IMADE Research Lab in the Institute of Science, Faculty of Applied Science at the Universiti Teknologi MARA Shah Alam, for generously providing laboratory facilities. The financial support from Universiti Teknologi MARA is gratefully acknowledged.

References

- 1. Ali, A. M. M., Subban, R. H. Y., Bahron, H., Winie, T., Latif, F., and Yahya, M. Z. A. (2008). Grafted natural rubber-based polymer electrolytes: ATR-FTIR and conductivity studies. *Ionics*, 14(6): 491-500.
- Aziz, S. B., Abdullah, O. G., Hussein, S. A., and Ahmed, H. M. (2017). Effect of PVA blending on structural and ion transport properties of CS:AgNt-based polymer electrolyte membrane. *Polymers*, 9(11): 622.
- Hamsan, M. H., Aziz, S. B., Nofal, M. M., Brza, M. A., Abdulwahid, R. T., Hadi, J. M., Karim, W. O., and Kadir, M. F. Z. (2020). Characteristics of EDLC device fabricated from plasticized chitosan:MgCl₂ based polymer electrolyte. *Journal of Materials Research and Technology*, 9(5): 10635-10646.
- Abdullah, O. G., Ahmed, H. T., Tahir, D. A., Jamal, G. M., and Mohamad, A. H. (2021). Influence of PEG plasticizer content on the proton-conducting PEO:MC-NH4I blend polymer electrolytes based films. *Results in Physics*, 23: 104073
- Majumdar, S., Mondal, A., Mahajan, A., Bhattacharya, S. K., and Ray, R. (2023). Dyesensitized solar cell employing chitosan-based biopolymer electrolyte. *IOP Conference Series: Materials Science and Engineering*, 1291(1): 012014.
- Abdulwahid, R. T., Aziz, S. B., and Kadir, M. F. Z. (2023). Environmentally friendly plasticized electrolyte based on chitosan (CS): Potato starch (PS) polymers for EDLC application: Steps toward the greener energy storage devices derived from biopolymers. *Journal of Energy Storage*, 67(5): 107636.
- Safavi-Mirmahalleh, S. A., Dadkhah-Janqor, A., and Salami-Kalajahi, M. (2024). Chitosan-based gel polymer electrolytes for high performance Li-ion battery. *International Journal of Biological Macromolecules*, 282: 137304.
- 8. Ponmani, S., Kalaiselvimary, J., and Ramesh Prabhu, M. (2018). Structural, electrical, and electrochemical properties of poly(vinylidene fluoride-co-hexaflouropropylene)/poly(vinyl

- acetate)-based polymer blend electrolytes for rechargeable magnesium ion batteries. *Journal of Solid State Electrochemistry*, 22(8): 2605-2615
- 9. Sampath Kumar, L., Christopher Selvin, P., and Selvasekarapandian, S. (2021). Impact of lithium triflate (LiCF₃SO₃) salt on tamarind seed polysaccharide-based natural solid polymer electrolyte for application in electrochemical device. *Polymer Bulletin*, 78(4): 1797-1819.
- Sanchez-Salvador, J. L., Balea, A., Monte, M. C., Negro, C., and Blanco, A. (2021). Chitosan grafted/cross-linked with biodegradable polymers: A review. *International Journal of Biological Macromolecules*, 178: 325-343.
- 11. Thakur, V. K., and Thakur, M. K. (2014). Recent advances in graft copolymerization and applications of chitosan: A review. *ACS Sustainable Chemistry and Engineering*, 2(12): 2637-2652.
- 12. Don, T. M., King, C. F., Chiu, W. Y., and Peng, C. A. (2006). Preparation and characterization of chitosan-g-poly(vinyl alcohol)/poly(vinyl alcohol) blends used for the evaluation of blood-contacting compatibility. *Carbohydrate Polymers*, 63(3): 331-339.
- 13. Chew, K. W. and Tan, K. W. (2011). The effects of ceramic fillers on PMMA-based polymer electrolyte salted with lithium triflate, LiCF₃SO₃. *International Journal of Electrochemical Science*, 6(11): 5792-5801.
- 14. Kingslin Mary Genova, F., Selvasekarapandian, S., Vijaya, N., Sivadevi, S., Premalatha, M., and Karthikeyan, S. (2017). Lithium ion-conducting polymer electrolytes based on PVA–PAN doped with lithium triflate. *Ionics*, 23(10): 2727-2734.
- Abdul Halim, N. J., Muhd Zailani, N. A., Nazir, K., Syed Ismail, S. N., and Abdul Latif, F. (2024). Effect of lithium triflate (LiTf) salt on the structural and electrochemical properties of the pectin-based solid polymer electrolytes films. Scientific Research Journal, 21(1): 145-162.
- Muhamad, S., Abdullah, S., Hashim, N. A. M. S. N., and Jalil, R. (2019). Characterization of solid polymer electrolyte using methylcellulose, KOH AND PEGD. Proceedings of the International Conference on Islamic Civilization and Technology Management, 23: 24.
- Aziz, S. B., Nofal, M. M., Abdulwahid, R. T., Kadir, M. F. Z., Hadi, J. M., Hessien, M. M., Kareem, W. O., Dannoun, E. M. A., and Saeed, S. R. (2021). Impedance, FTIR and transport properties of plasticized proton conducting biopolymer electrolyte based on chitosan for electrochemical device application. *Results in Physics*, 29(8): 104770.
- 18. El-hefian, E. A., Nasef, M. M., Yahaya, A. H.,

- and Khan, R. A. (2010). Preparation and characterization of chitosan/agar blends. *Journal of Chilean Chemical Society*, 55(1): 130-136.
- Nayak, P., Ismayil, Shetty, S. K., Sudhakar, Y. N., and Hegde, S. (2023). Unleashing the potential of eco-friendly chitosan: Methylcellulose polyblend electrolytes via magnesium acetate doping for solid state batteries. *Journal of Energy Storage*, 72: 108503.
- Kumar, A., Sharma, R., Suresh, M., Das, M. K. and Kar, K. K. (2017). Structural and ion transport properties of lithium triflate/poly(vinylidenefluoride-cohexafluoropropylene) -based polymer electrolytes. *Journal of Elastomers and Plastics*, 49(6): 513-526.
- Aziz, S. B., Asnawi, A. S. F. M., Mohammed, P. A., Abdulwahid, R. T., Yusof, Y. M., Abdullah, R. M., and Kadir, M. F. Z. (2021). Impedance, circuit simulation, transport properties and energy storage behavior of plasticized lithium ion conducting chitosan based polymer electrolytes. *Polymer Testing*, 101(7): 107286.
- 22. Aziz, S. B., and Abdullah, R. M. (2018). Crystalline and amorphous phase identification from the tanδ relaxation peaks and impedance plots in polymer blend electrolytes based on [CS:AgNt]x:PEO(x-1) (10 ≤ x ≤ 50). *Electrochimica Acta*, 285: 30-46.
- 23. Joshi, J. H., Kanchan, D. K., Joshi, M. J., Jethva, H. O., and Parikh, K. D. (2017). Dielectric relaxation, complex impedance and modulus spectroscopic studies of mix phase rod like cobalt sulfide nanoparticles. *Materials Research Bulletin*, 93: 63-73.
- Nayak, P., Sudhakar, Y. N., and Shetty, S. K. (2024). Charging toward sustainability: MgCl₂ doped chitosan–dextran polyblend electrolytes for energy storage device applications. RSC Advances, 14(50): 37045-37061.